

Platinum Coated Copper Nanowires and Platinum Nanotubes as Oxygen Reduction Electrocatalysts

Shaun M. Alia,^{†,‡} Kurt Jensen,^{†,‡} Christian Contreras,[‡] Fernando Garzon,[§] Bryan Pivovar,^{||} and Yushan Yan^{*,†,‡}

[†]Department of Chemical and Biomolecular Engineering, University of Delaware, Newark, Delaware 19716, United States

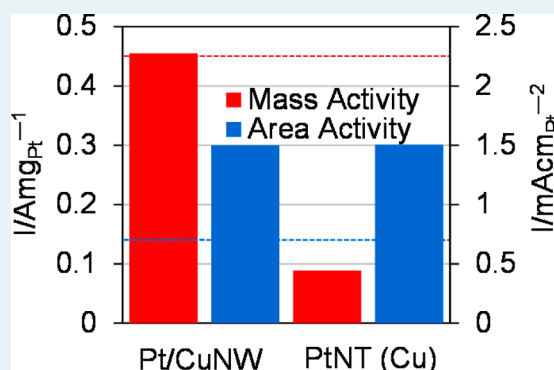
[‡]Department of Chemical and Environmental Engineering, University of California at Riverside, Riverside, California 92521, United States

[§]Los Alamos National Laboratory, Los Alamos, New Mexico 87545, United States

^{||}National Renewable Energy Laboratory, Golden, Colorado 80401, United States

S Supporting Information

ABSTRACT: Platinum (Pt) coated copper (Cu) nanowires (Pt/CuNWs) are synthesized by the partial galvanic displacement of Cu nanowires (CuNWs) with a Pt loading of 18 wt %. Pt/CuNWs have an outer diameter of 100 nm, a length of 25–40 μm , and a theoretical Pt layer thickness of 2 nm. Cu templated Pt nanotubes (PtNTs (Cu)) with a wall thickness of 11 nm, an outer diameter of 100 nm, and a length of 5–20 μm are synthesized by the complete galvanic displacement of CuNWs. CuNWs are synthesized by the hydrazine reduction of Cu nitrate in sodium hydroxide. Oxygen reduction reaction (ORR) and durability experiments are conducted on Pt/CuNWs, PtNTs (Cu), silver templated PtNTs (Ag), and carbon supported Pt nanoparticles (Pt/C) to evaluate catalyst activity for use as proton exchange membrane fuel cell cathodes. The ORR area activities of Pt/CuNWs and PtNTs (Cu) are 1.501 and 1.506 $\text{mA cm}_{\text{Pt}}^{-2}$, respectively. Pt/CuNWs produce a dollar activity of 9.8 $\text{A } \$^{-1}$ (dollar activity calculated from the DOE mass activity target for 2017–2020 of 0.44 $\text{A mg}_{\text{PGM}}^{-1}$). Durability testing of each catalyst shows improved retention of surface area and ORR activity in comparison to Pt/C.



KEYWORDS: proton exchange membrane fuel cells, platinum nanotubes, core shell catalysts

INTRODUCTION

The commercial deployment of proton exchange membrane fuel cells (PEMFCs) is limited by their catalysts' high cost and low durability.^{1,2} The development of catalysts with high activity for the oxygen reduction reaction (ORR) is essential to PEMFCs since the majority of activation losses occur at the cathode.^{3,4} Carbon supported platinum (Pt) nanoparticles (Pt/C) are typically utilized as the ORR catalyst but are inadequate for the combined cost, performance, and durability requirements. To promote the development of highly active ORR catalysts, the United States Department of Energy (DOE) set mass (0.44 A mg^{-1} , 2017–2020) and area (0.72 mA cm^{-2} , 2010–2015) activity targets.^{5,6} The durability of Pt/C is limited by the degradation of the carbon support and the loss of Pt surface area through Ostwald ripening, surface tension driven agglomeration, and potential driven dissolution and migration into the proton exchange membrane.⁷

Previous studies have examined Pt coated or Pt alloyed catalysts for improved ORR activity and/or reduced cost.^{8,9} Since the substrate or alloyed metal typically has a lower cost than Pt, normalizing activity to the total metal mass does not adequately demonstrate the cost savings this class of catalyst

offers. While this study completed ORR activity analyses in terms of total metal mass and Pt mass, dollar activities were also included to objectively quantify the cost benefit of Pt coated copper (Cu) nanowires (Pt/CuNWs). Dollar activities were derived as a cost normalized ORR mass activity and calculated using five year metal price averages (July 2006–2011) for Pt (\$ 1414.7 t oz^{-1}), Cu (\$ 6.3 t oz^{-1}), and silver (Ag, \$ 17.3 t oz^{-1}). In terms of dollar activity, the DOE mass activity target corresponded to 9.7 $\text{A } \$^{-1}$.

Previously, Ag nanowire (AgNW) templated Pt nanotubes (PtNTs (Ag)) were synthesized by galvanically displacing AgNWs and studied for ORR activity.^{9,10} Because of low surface area, PtNTs (Ag) are unable to meet the dollar target in their current form. Furthermore, Pt coated AgNWs are impractical as acidic ORR catalysts because of the strong antisegregation energy (theoretically 0.34 eV atom^{-1} for a Pt impurity on a Ag host).¹¹ The alloy formation does not allow a complete Pt shell and the presence of Ag is a liability for

Received: October 9, 2012

Revised: December 14, 2012

Published: January 22, 2013

corrosion first on the surface and then the bulk, eventually destroying the catalyst.

Xia et al. previously used Cu nanowire (CuNW) templated Pt nanotubes (PtNTs (Cu)) in the study of formic acid oxidation.¹² Although the activity of PtNTs (Cu) was significantly higher than Pt/C, the Pt utilization was low (PtNT wall thickness of 12 nm); furthermore, the templated growth directions were not preserved and ORR activity was not examined. PtNTs (Cu) were initially studied for ORR activity because of the low cost and facile synthesis of CuNWs in comparison to AgNWs. Preliminary analysis concluded that PtNTs (Cu) produced an area activity significantly larger than the DOE target and PtNTs (Ag). PtNTs (Cu), however, produced a dollar activity of 1.9 A \$⁻¹; to meet a dollar activity benchmark using a CuNW template, the Pt loading needed to be significantly reduced (to 19 wt % Pt) while maintaining a high ORR area activity. CuNWs further provide an acceptable substrate because Pt tends to segregate on a Cu surface (-0.04 eV atom⁻¹ for a Pt impurity on a Cu host), preventing Pt from migrating into the CuNW core.¹¹ In addition, Cu has a low dissolution potential (0.159 V) and can be easily removed electrochemically. Pt coated CuNWs (Pt/CuNWs) were therefore synthesized by the partial galvanic displacement of CuNWs. Pt loadings were optimized for catalyst cost and stability; the resulting Pt/CuNW catalyst examined in this study was found to be highly active and durable for ORR. This study was completed simultaneously with work performed by Pivovar et al. at the National Renewable Energy Laboratory on CuNW synthesis and the electrochemical characterization of PtNTs (Cu).^{13,14}

■ EXPERIMENTAL SECTION

CuNWs were synthesized by the hydrazine (N₂H₄, 35 wt %) and sodium hydroxide reduction of Cu nitrate in the presence of ethylenediamine (EDA), added to control wire morphology.¹⁵ In CuNW synthesis, a Cu nitrate solution (0.188 g in 10 mL of water) was added to 200 mL of 15 M sodium hydroxide in a 500 mL round-bottom flask. EDA was subsequently added to the flask (1.5 mL), followed by N₂H₄ (0.25 mL). Following each addition step, the flask was capped and shaken to evenly distribute the reactants. Once N₂H₄ was added, the flask was capped and placed in a 60 °C water bath for 1 h. Following the reaction, the flask contents were cooled in an ice bath and filtered. Filtering continued with excess water until the effluent reached a neutral pH. Prior to drying, the filter cake entered an argon environment. The CuNW synthesis method was similar to those previously published,¹⁵ with the difference that filtration was used to avoid the need of storing CuNWs in N₂H₄.

PtNTs (Cu) were synthesized via the galvanic displacement of CuNWs.¹² CuNWs (8.4 mg in 200 mL of water) were added to a 500 mL round-bottom flask equipped with an addition funnel, stir bar, and adapter passing argon. Following 15 min with flowing argon, chloroplatinic acid (0.036 g in 100 mL of water) was added dropwise over a period of 15 min. The flask proceeded for 1 h at room temperature to ensure a complete reaction. The PtNT (Cu) synthesis method was adopted from a previously published protocol,¹² but lower reactant concentrations were used to produce PtNTs (Cu) with desired templated growth directions.

Pt/CuNWs were synthesized via an incomplete galvanic displacement reaction with CuNWs. CuNWs (8.4 mg in 200 mL of water) were added to a 500 mL round-bottom flask, with

chloroplatinic acid (3.5 mg in 100 mL of water) in the addition funnel. Synthesis procedures of the Pt/CuNWs were identical to the aforementioned PtNTs (Cu). Although the displacement method was similar to those previously published,¹² no intentional partial displacement of CuNWs had been reported. Following synthesis, PtNTs (Cu) and Pt/CuNWs were washed in 1 M hydrochloric acid and water. Prior to electrochemical experiments, PtNTs (Cu) were annealed at 250 °C in forming gas (5% hydrogen, balance nitrogen) for 1 h. Pt/CuNWs were not annealed to prevent Pt–Cu alloying.

Scanning electron microscopy (SEM) images were taken at 20 kV with a Philips XL-30 FEG microscope. Transmission electron microscopy (TEM) images were taken at 300 kV with a Philips CM300 microscope. TEM samples were prepared on holey-carbon copper grids (Ted Pella, Inc.). The growth directions of PtNTs (Cu) and CuNWs were examined by selected area electron diffraction (SAED) at a length of 24.5 cm.

Rotating disk electrode (RDE) experiments were conducted in a 3-electrode cell equipped with a Ag/AgCl reference electrode, Pt wire counter electrode, and 5 mm diameter glassy carbon working electrode (Pine Instruments). Measurements were taken on a multichannel potentiostat (Princeton Applied Research), and the working electrode was fixed to a modulated speed rotator.

Nanotube and nanowire catalysts were dispersed in a water/isopropanol solution (water:isopropanol:: 3:1, by volume), forming a suspension with the concentration 0.392 mg mL⁻¹. A catalyst layer was formed on the working electrode by pipetting 50 μL of the catalyst suspension to reach a loading of 100 μg cm⁻². The theoretical catalyst layer thickness of PtNTs (Cu) was approximately 101 nm, calculated assuming the nanotubes aligned in a honeycomb stack. Because of differences in metal density, the theoretical catalyst layer thickness of Pt/CuNWs was approximately 82 nm. Pt/C was dispersed in a water/isopropanol solution (water: isopropanol:: 3:1, by volume) forming a suspension with the concentration 0.392 mg mL⁻¹. A catalyst layer was formed on the working electrode by pipetting 50 μL of the catalyst suspension to reach a loading of 100 μg cm⁻². Following the formation of the catalyst layer, 10 μL of 0.05 wt % Nafion (Liquion) in isopropanol was pipetted onto the working electrode to ensure catalyst adhesion to the glassy carbon electrode surface. Reference electrode values were converted to a reversible hydrogen electrode (RHE) with measurements between the Ag/AgCl reference and a bulk polycrystalline Pt (BPt) electrode in a hydrogen saturated 0.1 M HClO₄ electrolyte.¹⁶ Electrochemically active surface areas (ECSAs) were determined from the charge associated with hydrogen adsorption, assuming a value of 210 μC cm⁻². The validity of ECSA calculations were confirmed by examination of BPt, found to have a surface roughness of 1.2.

■ RESULTS AND DISCUSSION

Pt/CuNWs were synthesized with a diameter of 100 nm and a length of 25–40 μm (Figure 1 a–b). PtNTs (Cu) were synthesized with a wall thickness of 11 nm (as determined by high resolution TEM images), an outer diameter of 100 nm, and a length of 5–20 μm (Figure 1 c–d and Supporting Information, Figure S.1). The CuNWs used in the galvanic displacement had an outer diameter of 100 nm and a length of 40–50 μm (Supporting Information, Figure S.2). Previously synthesized PtNTs (Ag) had a wall thickness of 5 nm, an outer diameter of 60 nm, and a length of 5–20 μm.^{9,10} The Pt

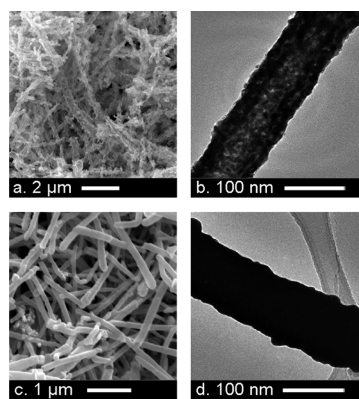


Figure 1. SEM and TEM images of (a–b) Pt/CuNWs and (c–d) PtNTs (Cu).

loading of Pt/CuNWs and PtNTs (Cu) was 18 wt % (total mass, 82 wt % Cu) and 95 wt % (total mass, 5 wt % Cu), respectively. Previously synthesized PtNTs (Ag) were also found to have a Pt content of 97 wt % (total mass, 3 wt % Ag). Pt loadings were determined by energy dispersive X-ray spectroscopy (EDS).

SAED patterns of CuNWs matched those previously found by Zeng et al. and confirmed the presence of single twinned CuNWs with growth in the $[1, -1, 0]$ direction (Supporting Information, Figure S.3).^{15,17} High resolution TEM images showed a $[1, -1, 1]$ lattice spacing of 0.25 nm (Supporting Information, Figure S.4). SAED patterns of PtNTs also matched the patterns of CuNWs provided by Zeng et al.¹³ The PtNTs therefore grew in the $[1, -1, 0]$ direction; high resolution TEM images confirmed a $[1, -1, 1]$ lattice spacing of 0.25 nm. The ability of Pt to maintain the growth directions and lattice spacing of CuNWs was in part attributed to matches in crystal structure and similar atomic size.

Catalyst ECSAs were determined during cyclic voltammograms in an argon saturated 0.1 M HClO₄ electrolyte at a scan rate of 20 mV s⁻¹ (Figure 2). ECSAs were calculated by the charge associated with hydrogen adsorption. ECSAs were

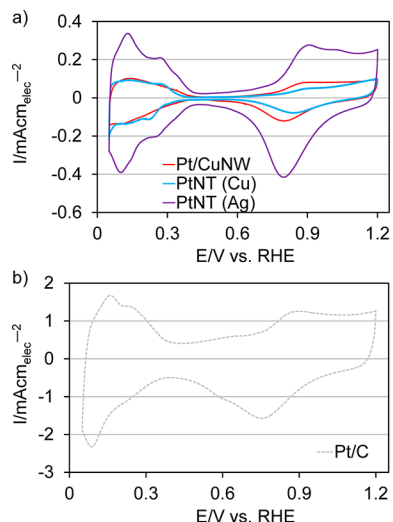


Figure 2. Cyclic voltammograms of (a) Pt/CuNWs, PtNTs (Cu), and PtNTs (Ag), and (b) Pt/C. Data was collected at 20 mV s⁻¹ in an argon saturated 0.1 M HClO₄ electrolyte. Cyclic voltammograms were presented as a function of electrode surface area.

further verified with the charge associated with carbon monoxide oxidation (Supporting Information, Figure S.5).¹⁸ Carbon monoxide oxidation voltammograms were performed by holding a potential of 0.2 V vs RHE for 20 min, the first 10 min in a carbon monoxide saturated electrolyte (10% carbon monoxide, balance nitrogen) and the second 10 min in an argon saturated 0.1 M HClO₄ electrolyte; following potential holding, a voltammogram was immediately performed at 20 mV s⁻¹. ECSAs for Pt/CuNWs, PtNTs (Cu), PtNTs (Ag), and Pt/C were determined to be 5.5, 5.6, 15.2, and 60.1 m² g⁻¹, respectively, on a total mass basis. On a Pt mass basis, Pt/CuNWs, PtNTs (Cu), PtNTs (Ag), and Pt/C had ECSAs of 30.6, 5.9, 15.7, and 60.1 m² g⁻¹, respectively. Pt/CuNWs had a much higher ECSA than PtNT (Cu) because of an increased Pt utilization. While PtNTs (Cu) had an 11 nm wall thickness, Pt/CuNWs were estimated to have an approximate Pt coating of 2 nm. Cu was also unstable during cyclic voltammetry and ORR experiments because of a low dissolution potential; because of the ease of electrochemically removing Cu, it was unlikely that Pt/CuNWs contained Cu impurities on the surface during ORR testing. Complete removal of Cu was further confirmed by the lack of Cu features in the cyclic voltammograms.

Pt/CuNWs, PtNTs (Cu), PtNTs (Ag), Pt/C, and BPt were examined for ORR activity with RDE experiments (Figure 3).

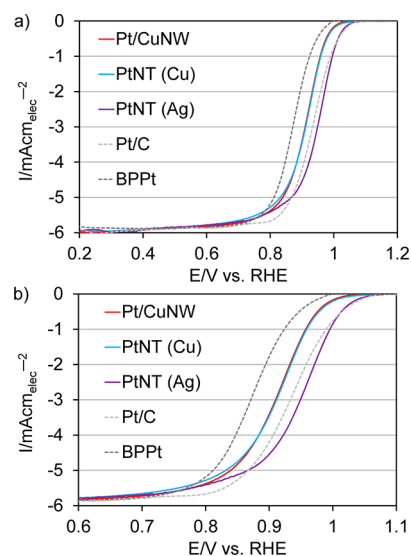


Figure 3. Anodic polarization curves of Pt/CuNWs, PtNTs (Cu), PtNTs (Ag), Pt/C, and BPt. ORR polarization curves were taken at 20 mV s⁻¹ and 1600 rpm in a 0.1 M HClO₄ electrolyte. Polarization curves were presented as a function of electrode surface area.

Kinetic activity was evaluated at 0.9 V vs RHE during anodic voltammograms at 1600 rpm and 20 mV s⁻¹ in an oxygen saturated 0.1 M HClO₄ electrolyte.^{19,20} Catalyst activity for ORR was normalized to the total metal mass (M), Pt mass (Pt), and dollar (Figure 4 and Supporting Information, Figure S.6). Pt/CuNWs produced a metal mass activity of 0.082 A mg_M⁻¹, within 97% of PtNTs (Cu). Pt/CuNWs further produced a Pt mass activity of 0.45 A mg_{Pt}⁻¹, 3.5% greater than the DOE Pt target. Pt/CuNWs exhibited a dollar activity of 9.8 A \$⁻¹, 1.4% greater than the dollar target, calculated from the DOE mass activity target. Catalysts were also evaluated in terms of area activity. Of particular interest was the large area activity of Pt/CuNWs and PtNTs (Cu), each exceeding the former DOE target by 2.1 times, Pt/C by 6.2 times, and

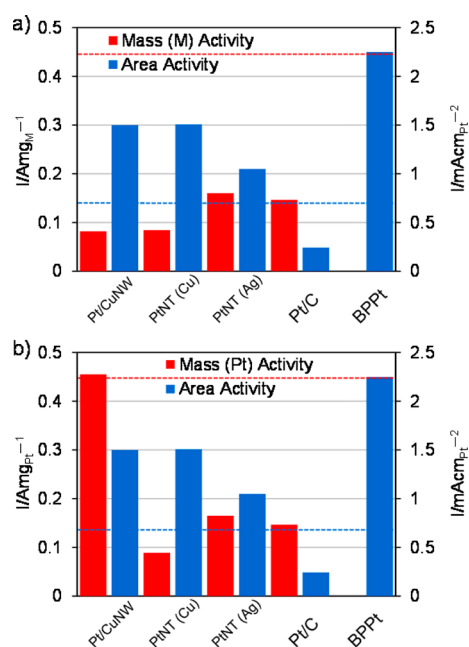


Figure 4. Activity normalized to Pt area, (a) total mass, and (b) Pt mass of Pt/CuNWs, PtNTs (Cu), PtNTs (Ag), Pt/C, and BPt; DOE targets are denoted by dotted lines. Catalyst activities were determined at 0.9 V vs RHE during ORR anodic polarization scans at 20 mV s^{-1} and 1600 rpm in a 0.1 M HClO_4 electrolyte.

reaching 77% the activity of BPt. Pt/CuNWs and PtNTs (Cu) further exceeded the area activity of PtNTs (Ag) by 43%.

Electronic tuning potentially contributed to the high area activity of Pt/CuNWs and PtNTs (Cu). The CuNW template and Cu alloying within the Pt layer introduced compressive strain, widening the Pt d-band and shifting the center further from the Fermi level; the d-band center shift weakened oxygen chemisorption, improving ORR activity.²¹ The d-band effect for Pt Cu systems was previously confirmed on the following: a Pt shell on Pt Cu nanoparticles;²² a Pt overlayer on Cu;²³ and a Pt Cu alloy.²³

The Pt growth directions potentially contributed to the high area activity as well. From the detailed analysis of growth direction by Xia et al. and Xie et al., PtNTs (Ag) similarly grew in the $\langle 110 \rangle$ and $\langle 111 \rangle$ directions, but were 5-fold twinned with a side surface dominated by the $\{100\}$ facet and higher indices in the $\langle 110 \rangle$ zone axis.^{24,25} In contrast, Pt/CuNWs and PtNTs (Cu) were single twinned with the side surface a statistical average of facets in the $\langle 110 \rangle$ zone axis. CuNWs, therefore, provided a better template for Pt ORR than AgNWs. The lower prevalence of the $\{100\}$ facet, the least active low index facet, contributed to a Pt/CuNW and PtNT (Cu) ORR area activity higher than that of PtNT (Ag).²⁶ The BPt electrode contains large grains, tens of micrometers in size, and is statistically an average of all low and high index facets. Since the side surface of Pt/CuNWs and PtNTs (Cu) did not contain the $\{110\}$ facet, the most active low index facet, the resulting ORR area activity was lower than that for BPt.²⁶

The ORR activity of catalysts was also determined as a function of area per dollar (Figure 5). The dollar activity target (9.67 $\text{A } \$^{-1}$), derived from the DOE mass activity target, was denoted by the solid line, indicating the area activity required at a given area per dollar. Activities to the upper right of the solid line indicated an ORR activity in excess of the dollar target. Although Pt/C produced the largest area per dollar (1.4 m^2

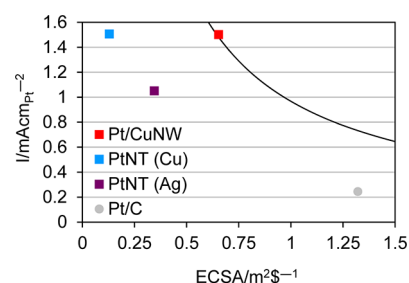


Figure 5. Pt area activity as a function of cost normalized surface area; DOE mass activity target denoted by a solid line. Catalyst activities were determined at 0.9 V vs RHE during ORR anodic polarization scans at 20 mV s^{-1} and 1600 rpm in a 0.1 M HClO_4 electrolyte.

$\text{A } \$^{-1}$), the area activity was insufficient to exceed the dollar target; an area per dollar of 4.0 $\text{m}^2 \text{ } \$^{-1}$ would be required to meet the dollar target at this area activity. While the area per dollar of PtNTs (Cu) was too low (0.1 $\text{m}^2 \text{ } \$^{-1}$), Pt/CuNWs increased the Pt utilization and area per dollar to 0.7 $\text{m}^2 \text{ } \$^{-1}$, thereby exceeding the dollar target.

Accelerated durability tests were conducted by potential cycling at 50 mV s^{-1} between 0.6 and 1.1 V vs RHE, with ECSA measurements taken every 6,000 cycles (Figure 6a). Pt/

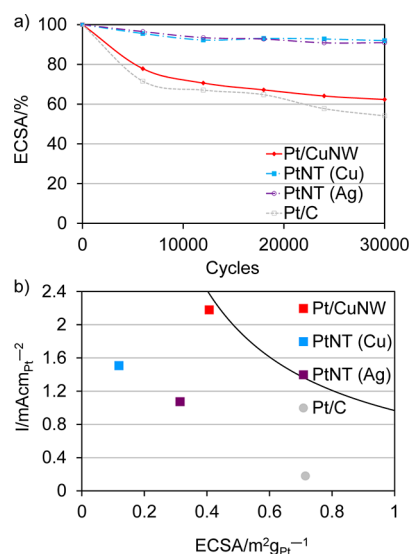


Figure 6. (a) ECSA loss of Pt/CuNWs, PtNTs (Cu), PtNTs (Ag), and Pt/C as a function of cycles in durability testing. (b) Pt area activity as a function of cost normalized surface area following durability testing; the dollar activity target, calculated from the DOE mass activity target, is denoted by a solid line. Catalyst activities were determined at 0.9 V vs RHE during ORR anodic polarization scans at 20 mV s^{-1} and 1600 rpm in a 0.1 M HClO_4 electrolyte. Durability testing was completed by potential cycling 30,000 times in the potential range of 0.6–1.1 V vs RHE at a scan rate of 50 mV s^{-1} .

CuNWs, PtNTs (Cu), PtNTs (Ag), and Pt/C retained 62.3%, 91.9%, 90.9%, and 54.1% of their original ECSAs, respectively, following 30,000 cycles. PtNTs (Cu) showed a significant durability improvement to Pt/C, attributed to the elimination of the carbon support and the extended network reducing Pt degradation and loss. In comparison to PtNTs (Cu), the ECSA retention of Pt/CuNWs decreased, attributed to the low dissolution potential of Cu. The high level of Pt/CuNW ECSA durability was attributed to the thickness of the Pt coating, largely preventing Cu exposure.

The area activities and area per dollar of Pt/CuNWs, PtNTs (Cu), PtNTs (Ag), and Pt/C were determined following durability testing (Figure 6b). Following 30,000 cycles, Pt/CuNWs produced an ORR dollar activity 91.7% of the dollar target, calculated from the DOE mass activity target, and 90.4% of pre durability Pt/CuNWs. Pt/CuNWs and PtNTs (Cu) further produced dollar activities 7.0 and 1.3 times of Pt/C. In terms of area activity, the Cu template catalysts exceeded the DOE target 2-fold to 3-fold.

CONCLUSIONS

Pt/CuNW catalysts have been synthesized and have area ORR activities of 1.5 mA cm⁻², significantly greater than Pt/C or PtNTs (Ag). The high area activity allowed for Pt/CuNWs to surpass the dollar activity target, derived from the DOE mass activity target, while expressing a surface area of only 5.5 m² g⁻¹. Pt/CuNWs further retained a greater proportion of surface area and ORR activity than Pt/C following durability testing, particularly noteworthy because of the use of the Cu substrate. The use of CuNWs is also more cost-effective than AgNW templates; the aqueous, low temperature synthesis of CuNWs and Pt/CuNWs is a significant benefit from the production perspective and can potentially make a larger impact in the commercialization of PEMFCs. Furthermore, Pt/CuNWs can lead to a thinner catalyst layer that is anticipated to improve Pt utilization and mass transport within the PEMFC.

ASSOCIATED CONTENT

Supporting Information

Supplementary figures. This material is available free of charge via the Internet at <http://pubs.acs.org>.

AUTHOR INFORMATION

Corresponding Author

*Fax: 302-831-2582. E-mail: yanys@udel.edu.

Notes

The authors declare no competing financial interest.

ACKNOWLEDGMENTS

This work was supported by the U.S. Department of Energy through the Fuel Cell Technologies Program under Contract No. DE-AC52-06-NA25396 with the Los Alamos National Laboratory and No. DE-AC36-08-GO28308 with the National Renewable Energy Laboratory.

ABBREVIATIONS

Cu; Pt; PtNT (Cu); CuNW; Pt/CuNW; ORR; DOE; PEMFC; Pt/C; Ag; AgNW; PtNT (Ag); N₂H₄; EDA; SEM; TEM; SAED; RDE; RHE; BPpT; EDS; ECSA.

REFERENCES

- (1) Borup, R.; Meyers, J.; Pivovar, B.; Kim, Y. S.; Mukundan, R.; Garland, N.; Myers, D.; Wilson, M.; Garzon, F.; Wood, D.; Zelenay, P.; More, K.; Stroh, K.; Zawodzinski, T.; Boncella, J.; McGrath, J. E.; Inaba, M.; Miyatake, K.; Hori, M.; Ota, K.; Ogumi, Z.; Miyata, S.; Nishikata, A.; Siroma, Z.; Uchimoto, Y.; Yasuda, K.; Kimijima, K. I.; Iwashita, N. *Chem. Rev.* **2007**, *107*, 3904.
- (2) Gasteiger, H. A.; Kocha, S. S.; Sompalli, B.; Wagner, F. T. *Appl. Catal., B* **2005**, *56*, 9.
- (3) Markovic, N. M.; Grgur, B. N.; Ross, P. N. *J. Phys. Chem. B* **1997**, *101*, 5405.
- (4) Paulus, U. A.; Schmidt, T. J.; Gasteiger, H. A.; Behm, R. J. *J. Electroanal. Chem.* **2001**, *495*, 134.

- (5) Bregoli, L. J. *Electrochim. Acta* **1978**, *23*, 489.
- (6) Kinoshita, K. J. *Electrochem. Soc.* **1990**, *137*, 845.
- (7) Darling, R. M.; Meyers, J. P. *J. Electrochem. Soc.* **2003**, *150*, A1523.
- (8) Stamenkovic, V.; Mun, B. S.; Mayrhofer, K. J. J.; Ross, P. N.; Markovic, N. M.; Rossmeisl, J.; Greeley, J.; Nørskov, J. K. *Angew. Chem.* **2006**, *118*, 2963.
- (9) Chen, Z. W.; Waje, M.; Li, W. Z.; Yan, Y. S. *Angew. Chem., Int. Ed.* **2007**, *46*, 4060.
- (10) Alia, S. M.; Zhang, G.; Kisailus, D.; Li, D. S.; Gu, S.; Jensen, K.; Yan, Y. S. *Adv. Funct. Mater.* **2010**, *20*, 3742.
- (11) Ruban, A. V.; Skriver, H. L.; Nørskov, J. K. *Phys. Rev. B* **1999**, *59*, 15990.
- (12) Lu, X.; McKiernan, M.; Peng, Z.; Lee, E. P.; Yang, H.; Xia, Y. *Sci. Adv. Mater.* **2010**, *2*, 413.
- (13) Pivovar, B. In *Annual Merit Review Proceedings*; U.S. Department of Energy - Hydrogen and Fuel Cells Program, 2011; http://www.hydrogen.energy.gov/pdfs/review11/fc007_pivovar_2011_o.pdf.
- (14) Pivovar, B. In *Annual Merit Review Proceedings*; U.S. Department of Energy - Hydrogen and Fuel Cells Program, 2010; http://www.hydrogen.energy.gov/pdfs/review10/fc007_pivovar_2010_o_web.pdf.
- (15) Chang, Y.; Lye, M. L.; Zeng, H. C. *Langmuir* **2005**, *21*, 3746.
- (16) Ives, D. J. G.; Janz, G. J. *Reference Electrodes, Theory and Practice*; Academic Press: New York, 1961.
- (17) Wiley, B. J.; Rathmell, A. R.; Bergin, S. M.; Hua, Y. L.; Li, Z. Y. *Adv. Mater.* **2010**, *22*, 3558.
- (18) Mayrhofer, K. J. J.; Strmcnik, D.; Blizanac, B. B.; Stamenkovic, V.; Arenz, M.; Markovic, N. M. *Electrochim. Acta* **2008**, *53*, 3181.
- (19) Takahashi, I.; Kocha, S. S. *J. Power Sources* **2010**, *195*, 6312.
- (20) Garsany, Y.; Baturina, O. A.; Swider-Lyons, K. E.; Kocha, S. S. *Anal. Chem.* **2010**, *82*, 6321.
- (21) Nørskov, J. K.; Rossmeisl, J.; Logadottir, A.; Lindqvist, L.; Kitchin, J. R.; Bligaard, T.; Jónsson, H. *J. Phys. Chem. B* **2004**, *108*, 17886.
- (22) Strasser, P.; Koh, S.; Anniyev, T.; Greeley, J.; More, K.; Yu, C.; Liu, Z.; Kaya, S.; Nordlund, D.; Ogasawara, H.; Toney, M. F.; Nilsson, A. *Nat. Chem.* **2010**, *2*, 454.
- (23) Ruban, A.; Hammer, B.; Stoltze, P.; Skriver, H. L.; Nørskov, J. K. *J. Mol. Catal. A: Chem.* **1997**, *115*, 421.
- (24) Sun, Y. G.; Mayers, B.; Herricks, T.; Xia, Y. N. *Nano Lett.* **2003**, *3*, 955.
- (25) Zhang, S. H.; Jiang, Z. Y.; Xie, Z. X.; Xu, X.; Huang, R. B.; Zheng, L. S. *J. Phys. Chem. B* **2005**, *109*, 9416.
- (26) Markovic, N. M.; Adzic, R. R.; Cahan, B. D.; Yeager, E. B. *J. Electroanal. Chem.* **1994**, *377*, 249.